Dalton Transactions

ROYAL SOCIETY OF CHEMISTRY

COMMUNICATION

View Article Online
View Journal | View Issue

Open Access Article. Published on 27 October 2025. Downloaded on 1/24/2026 6:32:03 PM.
This article is licensed under a Creative Commons Attribution 3.0 Unported Licence.

Check for updates

Cite this: *Dalton Trans.*, 2025, **54**, 15986

Received 24th September 2025,
Accepted 20th October 2025

DOI: 10.1039/d5dt02287h

rsc.li/dalton

Combined colourimetric and turn-on luminescence from a redox-switchable 2-aza-anthraquinone bridged dimetallic assembly

Alexandra R. Ibbott,[a] Peter N. Horton,[b] Simon J. Coles[b] and Simon J. A. Pope*[a]

A redox active 2-aza-anthraquinone unit was conjugated with 1,10-phenanthroline chelating units to give a dimetallic Ir(III) complex. The complex shows 'switch on' luminescence upon reduction of the azaanthraquinone bridge in turn revealing a highly visual colourimetric response.

The redox behaviour of anthraquinones (Scheme 1) attracts significant attention from researchers working in diverse fields. For example, anthraquinones have been investigated in the development of electrochemical sensors for DNA[1] and c-reactive protein,[2] in ionic liquid based electrochemical sensors for H_2O_2,[3] in thin film electrodes for reversible CO_2 capture,[4] and more recently in battery research,[5] including aqueous flow batteries.[6] The electronic properties of substituted anthraquinones also have a rich history in optical applications (anthraquinones were historically used as dyes and colourants in the textile industry[7]), including as components of colourimetric sensors[8] for a variety of analytes;[9] a number of studies detail metal ion coordination in anthraquinone species.[10]

Anthraquinones with amine substituents can display intramolecular charge transfer (ICT) absorption properties throughout the visible region (the position and number of amine substituents can tune the ICT band).[10] These optical properties are particularly attractive for colourimetric sensing applications.

Our ongoing interest in anthraquinone species relates to the subtle interplay between redox and optical properties, and the opportunities afforded by anthraquinones in the development of functional molecules. Specifically, we wanted to investigate the chemistry of 2-aza-anthraquinones (Scheme 1) in the development of colourimetric, redox-responsive compounds. Herein we report the design of a dimetallic Ir(III) complex that is bridged by a redox-active 2-aza-anthraquinone core. The resultant species demonstrate a redox-responsive, colourimetric and switch on luminescence behaviour in the visible region (Scheme 2). It is noteworthy that redox responsive probes are important in biological disciplines[11] where a fluctuating cell redox environment can help regulate cell cycle functions.[12]

The context for the current work is provided by previous studies on Ru(II) polypyridine complexes functionalised with quinone[13] or anthraquinone[14] moieties. These studies were motivated by interest in photoinduced electron transfer (PeT) processes and resultant charge separated states: PeT from the triplet metal-to-ligand charge transfer (^{3}MLCT) excited state of the Ru(II) unit to the accepting (anthra)quinone moiety can be energetically favourable. The extent of ^{3}MLCT quenching has been shown to be dependent upon the specific molecular structure of the assembly. Further, an ability to modulate the PeT quenching process, as demonstrated in a related Ru(II) complex, is a route to a tangible biological application focussed upon the study of hypoxia.[15]

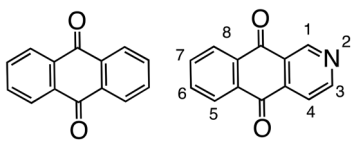

Scheme 1 Molecular structures of anthraquinone and the 2-aza-anthraquinone.

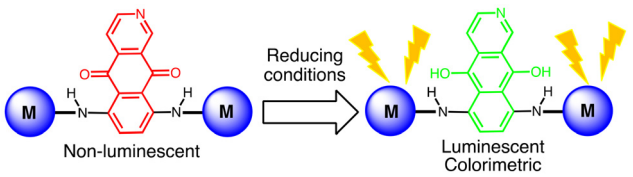

Scheme 2 Cartoon representation of the redox response of the 2-aza-anthraquinone bridged dimetallic complex.

[a]*School of Chemistry, Cardiff University, Main Building, Cardiff CF10 3AT, Cymru/Wales, UK. E-mail: popesj@cardiff.ac.uk*
[b]*UK National Crystallographic Service, School of Chemistry, University of Southampton, Highfield, Southampton, SO17 1BJ England, UK*

This journal is © The Royal Society of Chemistry 2025

Open Access Article. Published on 27 October 2025. Downloaded on 1/24/2026 6:32:03 PM.
This article is licensed under a Creative Commons Attribution 3.0 Unported Licence.

The target of the current work was to develop a molecule capable of a dual response to redox conditions, combining colourimetric and luminescent outputs.

Firstly, a new bridging ligand was synthesised (see SI for details) by heating two equivalents of 5-amino-1,10-phenanthroline with 5,8-difluoro-2-aza-anthraquinone in dry THF in the presence of excess NaH (Scheme 3). Over the course of three days a blue-coloured precipitate slowly formed and following filtration and chromatographic purification, a dark turquoise air stable powder, **L1**, was obtained in modest yield.

As the 2-aza-anthraquinone and 1,10-phenanthroline (phen) components are unsymmetrical, ^{1}H NMR spectroscopy was especially helpful to confirm the formation of the ligand. The furthest downfield signal was assigned to the N*H* resonances, which appeared as a coincident peak *ca.* 12.75 ppm (Fig. S1). A singlet resonance *ca.* 9.8 ppm was assigned to the 1-position of the 2-aza-anthraquinone. HRMS identified the $[M + H]^+$ and $[M + 2H]^{2+}$ ions at m/z = 596.1833 and 298.5957, respectively, while IR spectroscopy revealed the C═O stretches at 1562 and 1589 cm^{-1} (typical of diamino substituted anthraquinones[16] and shifted from 5,8-difluoro-2-aza-anthraquinone at 1676 cm^{-1}) as well as a broad N–H stretch at 3381 cm^{-1} (Fig. S2).

The solid-state structure of **L1** was categorically elucidated from single crystal X-ray diffraction (using dark blue, block-shaped crystals obtained from the diffusion of ^{i}Pr$_2$O into a CHCl$_3$ concentrate of **L1**). The data (Fig. 1) confirmed the expected structure and showed a torsional twist about the amine linkers that positions the 1,10-phenanthroline units out of the plane defined by the 2-aza-anthraquinone. Two intramolecular hydrogen bonding interactions are evident between the NH and C═O groups within each independent molecule. Data collection parameters are shown in Table S1, SI.

Complexation of **L1** was investigated using [Ir(ppy)$_2$(MeCN)$_2$]PF$_6$ [17] (where ppy = 2-phenylpyridine) to give the homo bimetallic complex **Ir2-L1** (Scheme 3). The ^{1}H NMR spectrum initially obtained at 293 K showed no evidence for free ligand, but was difficult to interpret due to the broadness of the resonances. A subsequent spectrum obtained at 353 K (in d6-DMSO) was more defined and well resolved (Fig. S3). The N*H* resonances now appeared as two distinct singlets at 12.3–12.4 ppm, and the characteristic singlet for the 1-position of the 2-aza-anthraquinone was clearly observed at 9.6 ppm. The other aromatic resonances associated with ppy and phen components were typically overlapping, but noted with the correct integrals. HRMS identified the doubly charged parent ion with an isotopic pattern that matched the theoretical distribution (Fig. 2). The IR spectrum confirmed the presence of the 2-aza-anthraquinone based carbonyl stretches around 1570–1600 cm^{-1} consistent with **L1** (Fig. S4).

As there is little literature on the electrochemical properties of 2-aza-anthraquinones, the redox properties of **L1** and **Ir2-L1** were compared to a relevant model compound, 5,8-bis(anilino)-2-aza-anthraquinone (see SI for details of its synthesis and full characterisation, Fig. S5–S7, including X-ray structure) and studied using cyclic voltammetry. Initially, the

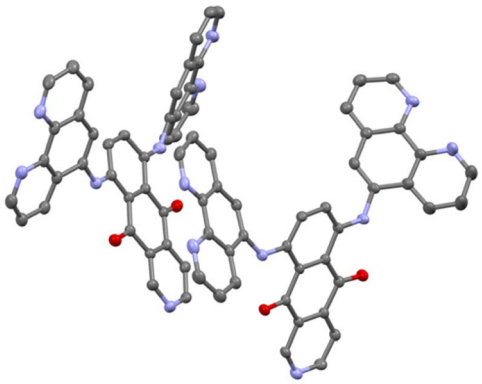

Fig. 1 X-ray crystal structure of **L1** (hydrogen atoms, and solvent of crystallisation removed; ellipsoids presented at 50% probability) showing the two independent molecules of the asymmetric unit.

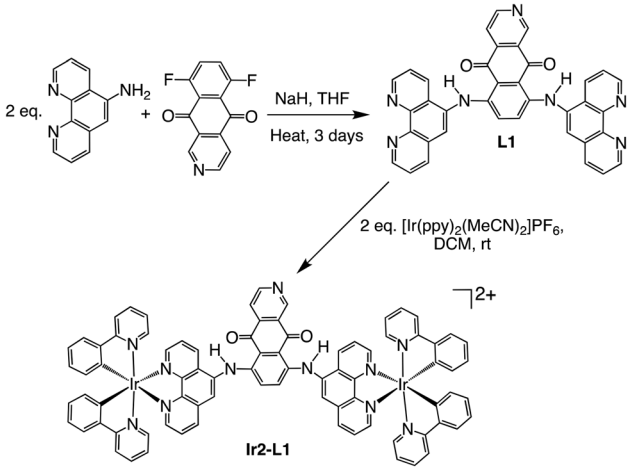

Scheme 3 Synthetic route to the 5,8-diamino-2-aza-anthraquinone bridged ligand, **L1** and the corresponding complex **Ir2-L1**.

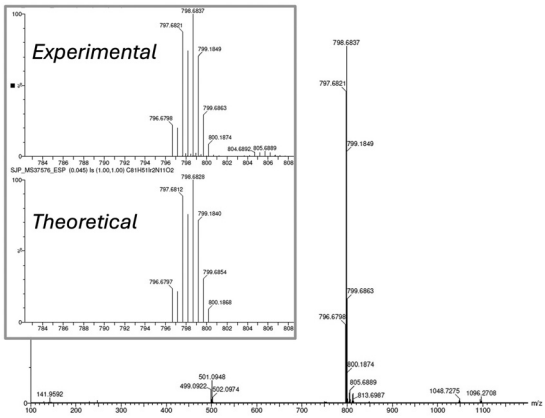

Fig. 2 Electrospray (positive), high resolution mass spectrum for **Ir2-L1** showing the cluster of peaks corresponding to the 2+ parent ion (inset provides comparison to the theoretical prediction).

Open Access Article. Published on 27 October 2025. Downloaded on 1/24/2026 6:32:03 PM.
This article is licensed under a Creative Commons Attribution 3.0 Unported Licence.

cyclic voltammogram of 5,8-difluoro-2-aza-anthraquinone showed two reversible features at −1.02 and −1.48 V (*vs.* Fc/Fc$^+$ = 0 V). The analogue of **L1**, 5,8-bis(anilino)-2-aza-anthraquinone, was then analysed and the first of these two reduction features was shifted to −1.18 V with a second feature around −1.55 V. Firstly this is closely comparable to amine substituted anthraquinones,[18] and secondly, is consistent with the 2-aza-anthraquinone becoming harder to reduce once the electron withdrawing fluorine groups have been replaced with aryl amine substituents. There was also an irreversible oxidation *ca.* +0.65 V, which is absent in 5,8-difluoro-2-aza-anthraquinone and was therefore tentatively assigned to oxidation of the secondary amine (*cf.* diphenylamine).[19] The electrochemical data for **L1** was very similar to 5,8-bis(anilino)-2-aza-anthraquinone and therefore the two reversible reduction features noted for **L1** can be attributed to 2-aza-anthraquinone localised redox processes (Fig. S8).

As expected, the cyclic voltammogram for **Ir2-L1** showed several overlapping contributions to the reduction waves (Fig. S9). The first reduction for **Ir2-L1** appeared at −0.93 V respectively and was not fully reversible, and tentatively assigned to a 2-aza-anthraquinone based process. This is consistent with complexation to Ir(III) that reduces the donating ability of the bridging amine groups and therefore the 2-aza-anthraquinone becomes easier to reduce. A further reduction feature is evident around −1.25 V (a ppy reduction is expected at more negative potentials[20]). In the anodic region, **Ir2-L1** showed two oxidation process at +0.61 and +1.0 V both of which were completely irreversible; these were assigned to the secondary amine group (*cf.* data for **L1**) and an Ir$^{3+/4+}$ process, respectively, and indicate electrochemical instability upon oxidation (Fig. S10).

The UV-vis absorption spectrum of **L1** (Fig. 3, inset) showed a strong and broad absorbance at 500–700 nm which can be attributed to a spin-allowed ($\varepsilon \sim 10\,000$ M^{-1} cm^{-1}) intramolecular charge transfer (ICT) transition localised on the amine-substituted 2-aza-anthraquinone core (a similar band was noted for 5,8-bis(anilino)-2-aza-anthraquinone – see SI).

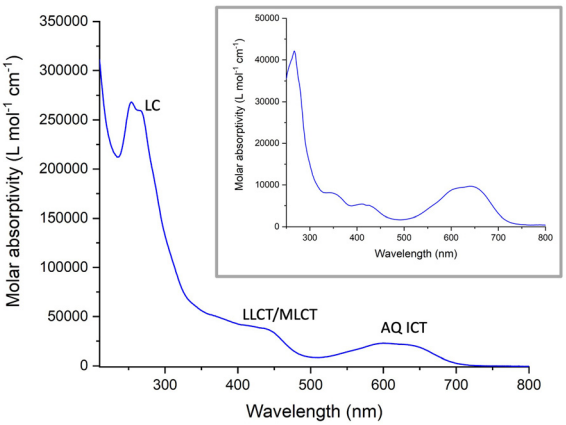

Fig. 3 UV-vis spectrum of **Ir2-L1** (MeCN). Note that 2-aza-anthraquinone ICT absorption dominates at 500–750 nm. Free ligand (**L1**) shown inset.

Additional absorption bands at 408, 344 and 267 nm are likely to be allowed $\pi \rightarrow \pi^*$ transitions located within the 2-aza-anthraquinone and phen fragments.

Upon complexation with Ir(III), the ICT of **L1** is added to the expected spin-allowed ^{1}LLCT/^{1}MLCT features that contribute at 380–475 nm, consistent with [Ir(ppy)$_2$(N^N)]$^+$ type complexes;[21] higher energy, overlapping, ligand-centred $\pi \rightarrow \pi^*$ transitions are also evident for this Ir(III) species. The wavelength complementarity of the visible absorption bands (Fig. 3) therefore provides the basis for the colourimetric response to redox state which is discussed later.

Photoluminescence studies on **Ir2-L1** showed that upon excitation (380 nm) in the ^{1}LLCT/^{1}MLCT region no observable emission was noted, which can therefore be attributed to very efficient quenching of the ^{3}MLCT excited state. As noted earlier, quinone type moieties can act as efficient quenchers of ^{3}MLCT excited states *via* thermodynamically favourable intramolecular electron transfer.

Since [Ir(ppy)$_2$(N^N)]$^+$ species are well-known excited state reductants (as well as oxidants), it is highly likely that PeT to the reducible 2-aza-anthraquinone unit is also feasible for **Ir2-L1**. The free energy of PeT (in eV) can be derived from $\Delta G_{\mathrm{PeT}} \approx E_{1/2}(\mathrm{D}^0/\mathrm{D}^+) - E_{1/2}(\mathrm{A}^0/\mathrm{A}^-) - E_{0-0}$ (where $E_{1/2}(\mathrm{D}^0/\mathrm{D}^+)$ is the oxidative potential of the donor; $E_{1/2}(\mathrm{A}^0/\mathrm{A}^-)$ is the reduction potential of the anthraquinone acceptor; E_{0-0} is estimated from the ^{3}MLCT emission profile in eV). For **Ir2-L1** the calculated value is estimated to be *ca.* −0.3 eV, and closely mimics the behaviour of previously reported Ru(II)/(anthra)quinone dyads.[13,14]

Having identified the electrochemical reduction features of **Ir2-L1**, UV-vis spectroscopy was then utilised to probe the optical ramifications of chemical reduction *via* the absorbance characteristics of **Ir2-L1**. $NaBH_4$ was selected as a relatively mild reducing agent (redox potential of −1.24 V *vs.* SHE at pH 14) and Fig. 4 clearly shows that sequential addition of a solution of $NaBH_4$ in isopropanol to a methanol solution of **Ir2-L1** leads primarily to a diminution of the longest wavelength ICT band. This is consistent with a reduction process that is 2-aza-anthraquinone localised since the loss of the electron deficient quinone core will deactivate the ICT transition. Spectrally this leads to a bleach of the 2-aza-anthraquinone ICT band between 500–700 nm. The colourimetric impact of this absorbance change is profound and shown in Fig. 5, whereby the reduced complex is yellow in appearance and evidently distinguishable from the native species (turquoise green) and free ligand (dark blue). The luminescence properties of **Ir2-L1** were then investigated under reducing conditions and showed a very clear switch on of the visible luminescence signal at 590 nm (observed lifetime 70 ns). While quite short (note that BH_4^- can also act as an excited state quencher), this lifetime value is still consistent with a phosphorescent ^{3}MLCT emission; the related complex [Ir(ppy)$_2$(bipy)]$^+$ has a lifetime of 275 ns in aerated MeCN.[21] It is noteworthy that superimposition of the absorbance spectrum of **Ir2-L1** and the emission spectrum of the reduced form of the complex demonstrate excellent overlap between the ICT and the ^{3}MLCT bands, which may

 This journal is © The Royal Society of Chemistry 2025

Open Access Article. Published on 27 October 2025. Downloaded on 1/24/2026 6:32:03 PM.
This article is licensed under a Creative Commons Attribution 3.0 Unported Licence.

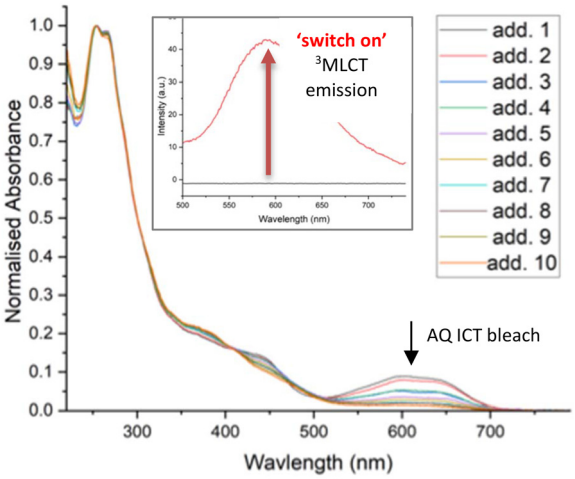

Fig. 4 Main: UV-vis spectra of the complexes showing the effect of adding $NaBH_4$ to **Ir2-L1** (10^{-5} M methanol). Inset: 'switch on' ^{3}MLCT luminescence (λ_{ex} = 380 nm) following reduction of **Ir2-L1**.

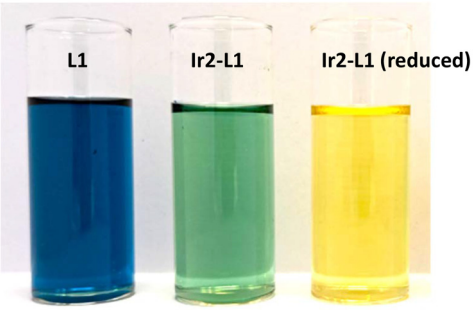

Fig. 5 Photograph showing the strong colour variance of methanol solutions associated with the free ligand, the Ir(III) complex and the reduced form of the complex (far right).

indicate that an energy transfer quenching pathway (spectral overlap integral calculated[22] as 2.8×10^{17} nm^4 M^{-1} cm^{-1}) is also viable for this system.

In summary, this study has shown that judicious choice of optically active molecular components can be assembled to give dual colourimetric and modulated luminescent output depending upon the redox environment. Future studies could consider the use of such compounds in sensing thin films where Ir(III) complexes have already shown great promise.[23] In that context, it will also be important to ascertain the redox cycling ability, and long-term stability, of the complex described herein. Given the well-established photophysical advantages afforded by phosphorescent metal complexes in bioimaging,[24] there will also be opportunity to scrutinise the biological application of such systems.

Conflicts of interest

There are no conflicts to declare.

Data availability

Data supporting this article have been included as part of the Supplementary information (SI). Supplementary information: experimental procedures, additional spectra, cyclic voltammograms and data collection parameters for X-ray crystallography. See DOI: https://doi.org/10.1039/d5dt02287h.

CCDC 2281059 (**L1**) and 2281060 (**5,8-bis(anilino)-2-aza-anthraquinone**) contain the supplementary crystallographic data for this paper.[25a,b]

Acknowledgements

We thank EPSRC for funding the PhD studentship of ARI (grant code: EP/L504749/1).

References

1 For example:J. Kongpeth, S. Jampasa, P. Chaupluk, O. Chailapakul and T. Vilaivan, *Talanta*, 2016, **146**, 318; E. M. Regan, A. J. Hallett, L. C. C. Wong, I. Q. Saeed, E. E. Langdon-Jones, N. J. Buurma, S. J. A. Pope and P. Estrela, *Electrochim. Acta*, 2014, **128**, 10; J. Rainbow, E. P. Judd-Cooper, S. J. A. Pope, N. J. Buurma and P. Estrela, *Sens. Diagn.*, 2025, **4**, 519.
2 S. Jampasa, W. Siangproh, R. Laocharoensuk, T. Vilaivan and O. Chailapakul, *Talanta*, 2018, **183**, 311.
3 P. Manusha, K. Theyagarajan, M. Elancheziyan, H. Shankar, K. Thenmozhi and S. Senthilkumar, *ECS Sens. Plus*, 2022, **1**, 033601.
4 D. Wieland, D. H. Apaydin and N. S. Sariciftci, *J. Mater. Chem. A*, 2018, **6**, 15095.
5 D. Werner, D. H. Apaydin, D. Wieland, K. Geistlinger, W. D. Saputri, U. J. Griesser, E. Drazevic, T. S. Hofer and E. Portenkirchner, *J. Phys. Chem. C*, 2021, **125**, 3745; D. G. Kwabi, K. Lin, Y. Ji, E. F. Kerr, M.-A. Goulet, D. De Porcellinis, D. P. Tabor, D. A. Pollack, A. Aspuru-Guzik, R. G. Gordon and M. J. Aziz, *Joule*, 2018, **2**, 1907; Y. Ji, M. A. Goulet, D. A. Pollack, D. G. Kwabi, S. Jin, D. Porcellinis, E. F. Kerr, R. G. Gordon and M. J. Aziz, *Adv. Energy Mater.*, 2019, **9**, 1900039.
6 M. Wu, N. Bahari, Y. Jing, K. Amini, E. M. Fell, T. Y. George, R. G. Gordon and M. J. Aziz, *Batteries Supercaps*, 2022, **5**, e202200009.
7 H.-S. Bien, J. Stawitz and K. Wunderlich, in Anthraquinone Dyes and Intermediates, *Ullmann's Encyclopedia of Industrial Chemistry*, Wiley-VCH Verlag GmbH & Co. KGaA, 2000.
8 For a review:A. Ghosh, D. A. Jose and R. Kaushik, *Sens. Actuators, B*, 2016, **229**, 545.
9 For example:L. Hou, X. Kong, Y. Wang, J. Chao, C. Li, C. Dong, Y. Wang and S. Shuang, *J. Mater. Chem. B*, 2017, **5**, 8957; K. Mariappan, P. K. Shrestha, A. Hussain and A. G. Sykes, *J. Mol. Struct.*, 2022, **1267**, 133585.

Open Access Article. Published on 27 October 2025. Downloaded on 1/24/2026 6:32:03 PM.
This article is licensed under a Creative Commons Attribution 3.0 Unported Licence.

10 E. E. Langdon-Jones and S. J. A. Pope, *Coord. Chem. Rev.*, 2014, **269**, 32.
11 D. R. Balce and R. M. Yates, *Redox Biol.*, 2013, **1**, 467.
12 A. I. Kostyuk, A. S. Panova, D. S. Bilan and V. V. Belousov, *Free Radicals Biol. Med.*, 2018, **128**, 23.
13 M. Borgstrom, O. Johansson, R. Lomoth, H. B. Baudin, S. Wallin, L. Sun, B. Akermark and L. Hammarstrom, *Inorg. Chem.*, 2003, **42**, 5173; A. C. Benniston, G. M. Chapman, A. Harriman and S. A. Rostron, *Inorg. Chem.*, 2005, **44**, 4029.
14 A. G. Bonn, O. Yushchenko, E. Vauthey and O. S. Wenger, *Inorg. Chem.*, 2016, **55**, 2894; M. Orazietti, M. Kuss-Petermann, P. Hamm and O. S. Wenger, *Angew. Chem., Int. Ed.*, 2016, **55**, 9407.
15 P. Zhang, H. Huang, Y. Chen, J. Wang, L. Ji and H. Chao, *Biomaterials*, 2015, **53**, 522.
16 J. E. Jones, B. M. Kariuki, B. D. Ward and S. J. A. Pope, *Dalton Trans.*, 2011, **40**, 3498; J. E. Jones and S. J. A. Pope, *Dalton Trans.*, 2009, 8421; J. E. Jones, A. J. Amoroso, I. M. Dorin, G. Parigi, B. D. Ward, N. J. Buurma and S. J. A. Pope, *Chem. Commun.*, 2011, **47**, 3374.
17 E. E. Langdon-Jones, B. D. Ward and S. J. A. Pope, *J. Organomet. Chem.*, 2018, **861**, 234.
18 D. Zarzeczanska, P. Niedzialkowski, A. Wcislo, L. Chomicz, J. Rak and T. Ossowski, *Struct. Chem.*, 2014, **25**, 625.
19 G. Inzelt, *J. Solid State Electrochem.*, 2002, **6**, 265.
20 A. B. Tamayo, B. D. Alleyne, P. I. Djurovich, S. Lamansky, I. Tsyba, N. N. Ho, R. Bau and M. E. Thompson, *J. Am. Chem. Soc.*, 2003, **125**, 7377.
21 S. Ladouceur and E. Zysman-Colman, *Eur. J. Inorg. Chem.*, 2013, 2985.
22 L. Burgess, H. Wilson, A. R. Jones, S. Hay and L. S. Natrajan, *Methods Appl. Fluoresc.*, 2020, **8**, 045003.
23 For example:M. Li, B. Zheng, D. Luo, H. Sun, N. Wang, Y. Huang, J. Dai, D. Xiao, S.-J. Su and Z. Lu, *Chem. Commun.*, 2015, **51**, 1926.
24 L. C.-C. Lee and K. K.-W. Lo, *Chem. Rev.*, 2024, **124**, 8825.
25 (*a*) CCDC 2281059: Experimental Crystal Structure Determination, 2025, DOI: 10.5517/ccdc.csd.cc2gkmk7; (*b*) CCDC 2281060: Experimental Crystal Structure Determination, 2025, DOI: 10.5517/ccdc.csd.cc2gkml8.

 This journal is © The Royal Society of Chemistry 2025